HHS Public Access

Author manuscript

Nat Neurosci. Author manuscript; available in PMC 2011 April 01.

Published in final edited form as:

Nat Neurosci. 2010 October ; 13(10): 1276–1282. doi:10.1038/nn.2630.

Intrinsic biophysical diversity decorrelates neuronal firing while increasing information content

Krishnan Padmanabhan[1,2] and **Nathaniel N. Urban**[1,2,3]

[1] Dept of Biological Sciences, Carnegie Mellon University, Pittsburgh, PA

[2] Center for the Neural Basis of Cognition, Pittsburgh, PA

[3] Department of Neuroscience, University of Pittsburgh, Pittsburgh PA

Abstract

While examples of variation and diversity exist throughout the nervous system, their importance remains a source of debate. Even neurons of the same molecular type show notable intrinsic differences. Largely unknown however is the degree to which these differences impair or assist neural coding. When outputs from a single type of neuron were examined - the mitral cells of the mouse olfactory bulb - to identical stimuli, we found that each cell's spiking response was dictated by its unique biophysical fingerprint. By exploiting this intrinsic heterogeneity, diverse populations coded for 2-fold more information than their homogeneous counterparts. Additionally, biophysical variability alone reduced pairwise output spike correlations to low levels. Our results demonstrate that intrinsic neuronal diversity serves an important role in neural coding and is not simply the result of biological imprecision.

Introduction

From the earliest drawings of neurons[1], to the identification of families of voltage-gated ion channels [2], a central theme of neuroscience has been the remarkable intrinsic variety of cells. While catalogues of *types of neurons* continue to grow [3], the importance of intrinsic diversity *within neurons of a single type* for neuronal coding has been largely ignored. Differences in channel expression and morphology [4], [5] can diversify spike outputs, even among cells of a single identified type [6]. Alternatively, spiking properties can be equivalent among neurons having channel densities in different proportions[6]. Intrinsic variability therefore seems to play multiple roles in mechanisms of spike generation. The extent to which these individual differences in cells are relevant to neural coding is however, less well understood.

Correspondence should be addressed to Dr. Nathan Urban, Department of Biological Sciences and Center for the Neural Basis of Cognition, 4400 Fifth Avenue, Mellon Institute, Room 173, Carnegie Mellon University, Pittsburgh, PA 15213. nurban@cmu.edu.

Supplemental information including detailed **methods, supplemental analysis** and **10 figures** accompany the paper.

Author contributions: K.P. conducted the experiments and the analysis. K.P. and N.U. wrote the manuscript.

The authors report that they have no competing interests.

Intrinsic diversity could play a critical role in neuronal coding, for example by reducing pairwise spike train correlations and reducing redundancy across populations of neurons, perhaps in conjunction with connectivity [7], [8]. Such decreases would afford populations of highly diverse neurons additional bandwidth with which to code for stimuli, as suggested by theoretical studies [9], [10]. But in noisy neural systems, where trial-to-trial variability is large[11], how the tradeoff between redundancy and bandwidth is balanced remains unexplored. At one extreme, biophysical differences may simply be the product of the imprecision of biology. For example, mosaic of neuronal properties may only reflect the probabilistic nature of gene expression among different cells. Alternatively, this diversity may be a functionally significant adaptation, whereby the noise of stochastic gene expression is harnessed in service of neuronal coding. Thus, understanding the effects of intrinsic diversity on neural responses and neuronal coding is essential for linking the cell biology of neurons with their functional role in information coding in the context of neuronal circuits. Heterogeneity in responses can arise from numerous sources, including anatomical differences and differences in inputs, but here we choose to focus on the mitral cells of the main olfactory bulb, where input correlations in mitral cells connected to the same glomerulus are high [12], and the anatomy is highly stereotypic.

Here we demonstrate that intrinsic biophysical diversity affects neuronal coding by reducing correlations in the population code while simultaneously increasing the information encoded by the population. We report two-fold increases in the coding capacity of populations of biophysically heterogeneous cells as compared to their homogeneous counterparts. This enhancement was seen both for random noisy inputs and for physiologically relevant stimuli modulated by oscillations corresponding to the frequency of sniffing. Additionally, we show that the spike triggered average (STA) can be used as one way to quantify neuronal diversity. Taken together, these data imply that biophysical heterogeneity is an important mechanism of robust population coding, not the unavoidable consequence of biology's imprecision.

Results

Mitral cells exhibit intrinsic biophysical diversity

To understand the role of intrinsic diversity in neuronal coding, recordings from mitral cells of the mouse main olfactory bulb *in vitro* were made (Fig. 1a). In the olfactory bulb, groups of ~ 25 mitral cells receive their excitatory input from the same population of several thousand olfactory receptor neurons (ORNs) in structures known as glomeruli [13]. Each glomerulus is the convergence point of all ORN axons expressing the same odorant receptor that together provide highly correlated inputs to mitral cells (Fig. 1a) [13], [14]. Mitral cells activated by the same odor in the same animal show different temporal responses [8], [15], [16]. In most cases, these responses are due to responses from mitral cells connected to different glomeruli [8]. In other examples however, highly variable responses are observed even when mitral cells are connected to the same glomerulus[17], suggesting that strongly correlated inputs trigger only *weakly* correlated outputs, not unlike what has been reported in neocortex [7], [18]. To explore differences in mitral cell intrinsic properties, a constant DC current was first injected into the mitral cell soma. This stimulus produced marked variability in mitral

cell output spike patterns (Fig. 1b-c, N = 34 cells, 19 animals). This variability was preserved in cells in which apical dendrites (green arrow) and lateral dendrites (blue arrow) were preserved, suggesting that spike pattern differences were not due to differences in morphology or to artifacts in slicing (N = 8). Analysis of these reconstructed mitral cells revlealed that they all had both apical and lateral dendrites (8/8), that 75% of cells (6/8) had well ramified apical tufts and 62.5% (5/8) had multiple obvious lateral dendrites extending throughout the bulb slice. The length of reconstructed dendritic processes totalled 1860±494 um (N = 8). Thus, although the cells were anatomically similar, they differed markedly in their firing patterns, including differences in the spike after-hyperpolarization (Fig. 1d).

Even neurons firing at similar rates (e.g. Fig. 1b-c black cell = firing rate 25 Hz, gray cell = firing rate 24 Hz) fired more or less regularly, as measured by the coefficient of variation (CV) of their interspike intervals (ISIs; black cell = 0.09 CV_{isi}, red cell = 1.12 CV_{isi}). These examples typified the variability seen across all mitral cells recorded (Fig. 1e, CV_{isi} = 0.44 ±0.33), and were indicative of the physiological signatures of their intrinsic biophysical differences [19], [20]. Furthermore, mitral cells had highly variable input-output functions (firing rate to a given DC input, Fig. 1f N = 11 cells).

Differential expression of voltage gated ion channels can lead to differences in intrinsic properties [6]. To characterize this differential channel expression, immunohistochemistry was performed on mitral cell populations against one subunit of the voltage gated potassium channel Kv1.2 (Fig. 1g). Examples of Kv1.2 positive mitral cells (Fig. 1g, red arrows) were directly next to cells that were Kv1.2 negative (Fig. 1g, white arrows), suggesting that one source of intrinsic diversity in the mitral cell population is the differential expression of the Kv1.2 subunit.

Mitral cell responses to complex stimuli are cell specific

Fixed DC current injection, as used above to identify regular spiking vs. bursting mitral cells (Fig. 1b-c) fail to capture the complex dynamics of neuronal firing[21]. To understand the effects of intrinsic diversity on neuronal output, mitral cell responses (in ACSF, containing 25 μM APV, 10 μM CNQX, 10 μM bicuculline to block fast synaptic transmission and isolate intrinsic properties) to identical rapidly fluctuating currents were recorded (Fig. 2a filtered Gaussian white noise black trace, σ = 40pA, DC = 100-400pA, N = 15 over multiple trials (n = 30-40 trials), Fig. S1). Because all synaptic transmission was blocked, differences in spike output were due to intrinsic biophysical variability. Identical experiments performed without blocking synaptic transmission showed similar results indicating that the differences identified were also present under different physiological conditions (data not shown).

Identical input noise triggered reliable spike trains in a single cell [22], [23], but the spike trains in different mitral cells varied considerably (Fig. 2a). To classify this output diversity, principal component analysis (PCA, Fig. S2) was performed on the spike trains. As there were no slow covarying elements in the first three principal components (Fig. S2), each cell's response reflected a differential filtering of the rapidly fluctuating current in the stimulus, rather than slow decorrelation or spike frequency adaptation. Projecting each spike train onto the first three principal components (Fig. 2b, each point is a trial, each color is a

cell condition) showed that while the across-cell responses were broadly distributed, within-cell responses were tightly packed.

To measure the similarities and the differences of spike trains within and between mitral cells in this space, each of the trials from the different recorded cells to the stimulus was classified using the k-nearest-neighbor (knn) algorithm. With only the first 15 principal components (3 nearest neighbors, using 60% of data for training), spike trains could be correctly classified as originating from a particular neuron with 86±2% accuracy (Fig. 2c, 20 resamples of data). Furthermore, the number of nearest neighbours (Fig. 2d), ranging from 1 to 10, did not affect classification accuracy (1 nearest neighbour = 86.7±2%, 10 nearest neighbours = 85.5±2%, P = 0.07 ANOVA) when 60% of the trials were used, suggesting that the clustering of spike responses was tight. Thus, a spike train from a single cell was more similar to the other spike trains from that cell than to spike trains from other cells. When changing the percentage of training vs testing data, a small effect on classification accuracy was observed (40% testing data gave 85.±3%, training accuracy, 80% testing data gave 88.8±3% accuracy, P = 0.006, ANOVA, Fig. 2e). Thus, the responses of all the trials in a single condition were highly reproducible and classification accuracy decreased only nominally when the number of trials used for training was reduced by half. Consequently, spike trains to the identical stimulus were reliable across trials in one cell, but specific across all cells.

Intrinsic diversity reduces correlations in spike output

Correlated spiking can emerge as a result of reliable firing among populations of cells that are driven by inputs that are highly correlated [17]. However, intrinsic diversity may reduce pairwise correlations between cells. To explore this question, correlations of spike trains across all trials in the same cell and between trials in different mitral cells to this identical input were calculated (Fig. S3). Spike train correlations across trials recorded from a single cell were high (Fig. 3a, black within-trials example, gray between-trials for the different cells), but were much lower between the trials of different cells (Fig. 3a inset, within cell R^2 = 0.17±0.002, between cell R^2 = 0.04±0.00, N = 15, P = 3.7×10^{-10}). When pairwise correlations across all trials from all cells to the stimulus were compared (N = 589 trials, 30 - 40 trials/condition), the mean was R^2 = 0.08±0.09 (Fig. 3b).

Thus, the intrinsic differences between this population of mitral cells reduce correlations of mitral cell responses to fluctuating inputs. The pairwise similarity between spike trains was low even when the inputs that drove those spikes were perfectly correlated. Low output correlations were not due exclusively to differences in firing rate; near-zero correlations were observed even with similar firing rates (Fig. 3c, gray arrow). Furthermore, when the precision by which correlation was measured was relaxed, pairwise population correlations were still only 0.34±0.15 for a 16 ms window (Fig. S3). Thus, intrinsic diversity between mitral cells *alone* was sufficient to reduce correlations between neural spike trains.

Diversity can be described by analysis of STAs

Rapidly fluctuating stimuli [21], in addition to providing an input for assessing correlation [23], can be used to probe the complex features of a cell's intrinsic dynamics [24]. To explore this

further [11], [22], [23], [25], a family of rapidly fluctuating currents that differed in their variance and DC offset (Fig. S1, σ = 20-80 pA, DC = 100-600 pA) was injected into a population of recorded mitral cells, where all excitatory and inhibitory synapses were blocked (25 μM APV, 10 μM CNQX, 10 μM bicuculline). Additionally, identical experiments were performed where synaptic activity remained and found highly similar results. To characterize the features of the stimulus to which each neuron responded, the average stimulus waveform preceding all the spikes in that neuron, a quantity called the spike-triggered average (STA, Figs. S4-S5, [24], [26 27]) was calculated for each cell. Differences in STAs indicated that different mitral cells were filtering different features of the stimulus, and the different filters reflected differences in the biophysical properties of these neurons [24]. The STAs (Fig. 4a) of the 3 cells in figure 2a were highly variable, representative of the heterogeneity in stimulus filters across all the mitral cells that were recorded (Fig. 4b, N = 35 STAs). To analyze these filters, principle component analysis (PCA) was done on the STAs (Fig.S4), allowing each STA to be represented as a linear combination of PCs [28]. The first three components (Fig. 4c) accounted for 90% of the STA variance (Fig. 4d), and their projection into the space defined by these components (Fig. 4e) showed that STAs were not uniformly distributed, and that diversity was preserved across multiple firing rates (Figs. S4-S5). Consequently, STA shapes projected onto the space defined by the first three principal components allowed us to visualize the distribution of intrinsic biophysical variability.

Biophysical diversity predicts information gain

To connect intrinsic diversity (STA) to information coding, spike trains were evoked in many neurons at different DC values (N = 15) using a rapidly fluctuating *identical stimulus* [21], [23] over multiple trials (N = 30-70 trials, 6 trials/cell are shown in Fig 5a, Fig. S1). This can be seen as analogous to the case in which groups of mitral cells receive highly similar inputs from the same population of sensory receptor neurons [14]. As all mitral cells received identical input fluctuations and all synaptic activity was blocked, differences in spike output were the result of intrinsic biophysical diversity. From these recordings, homogeneous (N = 45 populations/network size) and heterogeneous populations (N = 200 populations/network size) were generated ranging in size from 2-10 mitral cells to explore the connection between diversity and entropy/information in spike output (Fig. 5b, Fig. S6 [29]). Homogeneous population responses were made by drawing spike trains from the set of trials recorded in a *single neuron* (Fig. 5b, blue cell), equivalent to the case where a stimulus was encoded by *identical cells* receiving the *same input*. By contrast, heterogeneous responses were created by selecting groups of *non-identical neurons* from the population of all recorded cells (Fig. 5b, 4 cells in the example). Spike trains recorded on individual trials for each of these different cells (Fig. 5b) were then drawn randomly to create the heterogeneous response (Fig. 5b), analogous to a case where biophysically distinct cells process the same input (N = 2000 trials/network Fig. S7 [29]). When the number of neurons in the population was small (e.g. 2 cells, Fig. 5c), only small differences between the information transmitted by the homogeneous population (0.60±0.15 = bits/8 ms bin) and the heterogeneous population (0.71±0.12 bits/8 ms bin) could be identified. However, as population size grew, heterogeneous networks (red, Fig. 5c) quickly carried more information than their homogeneous counterparts (black, Fig. 5c). Gains increased up to 2.1-fold (Fig. 5c, Fig. S7) in the largest network examined (10 mitral cells), where heterogeneous populations carried

2.66±0.12 bits/8 ms, significantly more than homogeneous populations of the same size (1.27±0.07 bits/ms), ($P < 5\times10^{-7}$ ANOVA).

To determine if biophysical diversity accounted for the increases in information, the population's STA diversity was related to information for each set of heterogeneous mitral cells (Fig. 6, N = 1800 different simulated populations). Representative trials selected at random from the responses of each cell in one example of a heterogeneous mitral cells are shown for a 10 cell population (Fig. 6a). The STAs of each neuron (Fig. 6b) were then used as a measure of that mitral cell's intrinsic diversity contribution to the population. From this pairwise distances between these STAs (Fig. 6c) in the principal component space defined in Fig 4 could be calculated. As the mitral cell population's STA diversity increased, the bits of stimulus information relayed by those populations continued to increase to 2.60±0.16 bits/8 ms (Fig. 6d, $R^2 = 0.89$, N = 1800). Thus, the more intrinsically diverse the population, the more information the ensemble of mitral cells conveyed (Fig. 6d, Figs. S8-S9).

Diversity increases information during oscillatory inputs

In mammals, inputs to mitral cells are strongly modulated by oscillatory drive, corresponding to the animal's sniffing cycle (1-10 Hz in mice), and this periodic sampling of odours is thought to be essential for behaviour and the processing of odour information [30], [31]. To determine if the gain in information conferred by biophysically heterogeneity was present when mitral cells received physiologically relevant stimuli, mitral cells were injected with both synaptic barrages generated by convolving a random spike train with an alpha functions and synaptic barrages modulated with an underlying 8 Hz oscillation (Fig. 7a, Fig S10, N = 11 cells w/theta, N = 23 cells total). Spike trains from mitral cells (N = 27-40/cell) presented with an identical synaptic or synaptic + 8 Hz current were collected over multiple trials in both of these conditions. Again, these two conditions could be thought of as the case when populations of mitral cells receive highly similar synaptic inputs modulated by sniffing from groups of sensory neurons expressing the same olfactory receptor proteins. Responses for 3 mitral cells to the identical input are shown (Fig. 7b) along with the probability of spiking throughout the stimulus for each of the cells (Fig. 7c). The underlying theta rhythm resulted in locking of spike patterns to specific phases of the oscillation [32], notably in this example to the rising phase and the peak (Fig. 7c). However, when the precise timing of spikes in these cells was examined, differences quickly became apparent (Fig. 7d-e). Specifically, even mitral cells firing at similar rates (cell 1 =11.5±1.9 Hz, cell 2 =8.6±2.1 Hz, cell 3 =13.7±1 Hz) showed considerable heterogeneity with spike times for each neuron staggered throughout various phases of the oscillation (Fig. 7d). In the highlighted epoch for instance (Fig. 7d), cell 3 (in blue) fired first, and was followed by cell 1 (in black) and then cell 2 (in red) (Fig. 7e). When the STAs of these three different mitral cells was calculated by injecting a noisy stimulus, (Fig. 7f), they were indeed different. Thus the STA, in addition to reflecting each neuron's unique biophysical fingerprint, also reflected the diversity of that neuron's spike timing across various phases of an input driven by strong theta oscillatory activity. To determine the extent to which these differences in spike timing across theta cycles allowed mitral cells to code for information, model populations of homogeneous and heterogeneous neurons were created as before (Fig. 6a) from cells that all

received the same synaptic input and the same synaptic input modulated by a theta oscillation.

For synaptic inputs, 8 cell heterogeneous populations (N = 100) carried 1.67±0.13 bits/8 ms, significantly more ($P = 1.3 \times 10^{-30}$, ANOVA) than their 8 cell homogeneous network (N=11) counterparts, which carried only 0.91±0.3 bits/8ms). Perhaps most significantly however, 8 cell heterogeneous networks (N = 100) that received synaptic inputs which rode on top of an underlying 8 Hz oscillation carried 24.5±2.5 bits/sniff, significantly more ($P = 5.1 \times 10^{-24}$, ANOVA) that the information carried by 8 cell homogenous networks (12.6±5.8 bits/sniff, N = 11). Taken together, these data suggest that biophysically heterogeneous populations of mitral cells can code for up to 1.9 fold more information per sniff cycle as compared to biophysically homogeneous populations of mitral cells. Furthermore, the degree of biophysical heterogeneity as measured by STA diversity correlated with the gains in information across different types of physiologically relevant stimuli (Fig. S10). Therefore, the coding capacity gains associated with diverse populations of mitral cells appeared to be preserved across a host of conditions, ranging from noisy stimuli to synaptic inputs modulated by a strong 8 Hz oscillation. In sum, the computational advantages conferred by intrinsic biophysical heterogeneity are a general feature of neural coding across a range of physiologically relevant stimuli.

Discussion

The origin and importance of intrinsic diversity

While neurons have long been known to be diverse in their anatomical and physiological properties. [3], [33], our results are the first to demonstrate the importance of *intrinsic biophysical diversity* in a population of neurons (mitral cells of the olfactory bulb) believed to be highly homogeneous, and shown to receive highly correlated inputs [14]. A neuron's response to incoming stimuli is shaped by the voltage-gated ion channels expressed in that cell [34], [35]. Different combinations of these channels may generate functional differences or may result in a population of neurons that are physiologically similar despite being molecularly different [6], [36]. Consequently, the diversity that emerges from individual differences in gene expression [37] in some cases appears to be nullified by the combinatorial expression of different channels in that cell. In such instances, intrinsic diversity is titrated to produce equivalent output responses [6]. In other cases, populations of inhibitory [3] and excitatory [33], [38] neurons both in the mammalian neocortex and inhibitory neurons in the Drosophila olfactory system [39] also exhibit a remarkable intrinsic diversity. In these regions, and these populations of neurons, differences in the expression of ion channels and morphology result in the marked heterogeneity of the intrinsic properties of those cells [39], and thus the responses are diverse even when similar inputs are delivered[33].

While a number of mechanisms have been proposed to account for the *origin and extent* of these intrinsic differences [40], we demonstrate in this work the *role* that differences in intrinsic biophysical heterogeneity can play in neural coding.

The effect of intrinsic diversity on correlations

One aspect of coding where heterogeneity may be important is in correlated activity among populations of cells [41]. Correlations in output spiking can occur as a result of cells receiving highly correlated inputs [12], but these output correlations are often substantially less than the input correlations [17], due to a number of factors [8], including active decorrelation due to network connections [7], [42]. Although the degree and origin [17] of this correlated firing remains controversial [7], [18], our results demonstrate that intrinsic diversity alone is sufficient to erode output correlations even when inputs are shared and even when only a single population of neurons is considered. Precise correlations have been identified as playing a crucial role in a number of systems, including the olfactory bulb [43]. In the antenna lobe, the insect analog of the mammalian olfactory system, spiking activity is synchronized by 20 Hz oscillations [44], and desynchronization of this activity degrades the odor representation and impairs discrimination [45]. Our results also suggest that intrinsic biophysical diversity among mitral cells may reduce the degree to which firing is correlated even when incoming ORN excitatory inputs are very similar and gated by oscillatory drive. In mammals, where respiratory drive and sniffing produce strong oscillatory input in the theta frequency, diverse cells may exploit their intrinsic differences to spread spikes across various phases of the underlying respiratory cycle, improving the information coding capacity of the population as we have shown.

Diversity of intrinsic properties may also influence the extent to which mitral cells can be synchronized by aperiodic inhibition [46]. Reciprocal interactions between mitral cells and the inhibitory population of granule cells to which they are connected may be an additional source of diversity which can dynamically [42] alter the correlational structure of the spike outputs [47]. In this respect, important relationships could exist between the dynamics of individually heterogeneous cells and the networks in which they are embedded.

Intrinsic diversity's role in neuronal coding

Among the many approaches taken to examine questions of neural computation, biophysical models of single neurons, and statistical analysis of populations of neurons have both been powerful. Dynamical systems approaches have provided insight into how single neurons and networks respond to stimuli [11]. Simultaneously, the statistical characterization of neuronal responses and neuronal variability has allowed descriptions of neural computation in terms of the functions being performed[21], [29]. Largely absent however, is a framework that relates diversity in the parameters for spike generation in a single neuron with the coding of a population of neurons comprised of these diverse individual cells. Building on our previous work [24] showing how the STA, a concept in neural coding, is related to the phase resetting curve (PRC), an idea from neuronal dynamics, we demonstrate here how diversity at the single cell STA level (and by extension, the single cell PRC) contributes to efficient population coding. Our data establish a bridge linking these two frameworks, connecting the dynamical systems perspective (PRC–>STA) of a single neuron with the statistical perspective of a population code (STA–>bits). Thus, population coding may not simply the product of more neurons, or more connections, but depends on the contributions of intrinsic biophysical diversity to tie these elements together.

Materials and methods

Animal Procedures

All procedures were done in accordance with the guidelines for the care and use of animals at Carnegie Mellon University and as previously described[48, 49]. Briefly, C57Bl/6 mice between P11 and P19 were deeply anesthetized with isoflurane and then decapitated. Brains were removed and placed in ice-cold Ringer's solution (concentrations in mM = 125 NaCl, 25 Glucose, 2.5 KCl, 25 $NaHCO_3$, 1.25 NaH_2PO_4, 1 $MgCl_2$, and 2.5 $CaCl_2$). Coronal sections 300 um in thickness were made of the main olfactory bulb using a vibratome (VT1000S, Leica, Nussloch, Germany). After cutting, slices were incubated in Ringer's solution of (concentration in mM = 125 NaCl, 25 Glucose, 2.5 KCl, 25 $NaHCO_3$, 1.25 NaH_2PO_4, 1 $MgCl_2$, and 2.5 $CaCl_2$) at 37°C for 30 minutes before recordings were made.

For immunohistochemistry, mouse tissue was extracted from animals at P20. Briefly, animals were deeply anesthetized and then perfused with a solution of 4% paraformaldahyde and 30% sucrose in 0.1 phosphate buffer. 50 μm saggital sections of the main olfactory bulb were then made for subsequent processing.

Electrophysiology

Whole-cell recordings were made using patch pipettes filled with an internal buffer (concentration (130mM potassium gluconate, 10mM HEPES, 2mM $MgCl_2$, 2mM MgATP, 2mM Na_2ATP, 0.3mM GTP, 4 mM NaCl and in some cases 10-50 uM Alexa 488/594 Hydrazide or 1% biocytin) using a Multiclamp 700A amplifier (Molecular Devices, Palo Alto, CA) and an ITC-18 data acquisition board (Instrutech, Port Washington, NY). Mitral cells were identified under infrared differential interference contrast optics based on their laminar position in the olfactory bulb and their morphology. Cell identity was confirmed with fluorescent intracellular fills that revealed clear apical dendrites that ramified into a single glomerulus. Current clamp recordings were performed using whole-cell patch pipettes. All experiments were done at 35 °C in Ringers solution (concentrations in mM = 125 NaCl, 25 Glucose, 2.5 KCl, 25 $NaHCO_3$, 1.25 NaH_2PO_4, 1 $MgCl_2$, and 2.5 $CaCl_2$) with excitatory (25 uM APV and 10 uM CNQX) and inhibitory (10 uM Bicuculline) synaptic activity blocked. Additional experiments performed without synaptic blockers were done with Ringers solution as described above except with a $MgCl_2$ concentration of 0.2 mM. For all recordings, a 25 pA or 50 pA hyperpolarizing pulse was injected before stimuli were delivered to measure input resistance and membrane time constant, allowing us to track the stability of recordings over multiple trials. When multiple stimuli were presented to mitral cells, trials were interleaved to prevent systematic differences in neural responses that may have arisen over the entire recoding epoch.

Immunohistochemistry

A monoclonal antibody against a subunit of the voltage gated K^+ channel was used to characterize differences in channel expression. The monoclonal antibody Kv1.2 was developed by and obtained from the UCDavis/NIH NeuroMab Facility, supported by NIH grant U24NS050606 and maintained by the Department of Neurobiology, Physiology and Behavior, College of Biological Sciences, University of California, Davis, CA 95616. The

primary Kv1.2 antibody was used at a dilution of 1:1000 for 1 hr. The secondary of donkey anti-mouse Alexa-Fluor 488 (Invitrogen, CA), was used at a 1:600 dilution for 1 hr. For all sections, an additional Hoechst stain to identify cell nuclei was used. Sections were then imaged using a confocal microscope by scanning multiple regions of interest (ROIs) in both the bulb and the mitral cell layer.

Stimulus

Noise traces were generated as previous described [23]. Briefly, a 2.5 second white noise current was convolved with an alpha function having a 3 ms rise time (Fig S1a, top trace). The alpha function was selected as it reflected the time scale for optimal reliability of mitral cell spiking to a fluctuating input [23]. In Fig S1a, the identical input in the top trace was delivered to all the cells causing differences in spiking responses; including different rates of firing in each cell and different times at which individual spikes occurred even when firing rates were similar (Fig S1a bottom traces, each color represents a cell, each raster a trial). Representative examples of responses to different noise stimuli for another group of cells (Fig S1b) illustrates that the response diversity identified (firing rates, spike times, ISI of spikes, etc) were present over various types of stimuli, suggesting that the variability in neuronal responses reflected underlying intrinsic differences across a host of stimuli rather than differences highlighted by selecting a single stimulus.

The variance of the noise used was between 5% and 40% of the DC (100 pA-800 pA, σ = 20 pA-80 pA) offset for each cell with the majority of cells receiving 10-20% offset (Fig. S1c-d). The variance of the noise was selected as previously described [23], [24] to allow for appropriate estimation of the spike triggered average. Specifically, the noise values chosen induced reliable firing in neurons without large input fluctuations. The input fluctuation values chosen were sufficiently small that there was poor correlation between the σ of the input noise and the degree of reliability (R = 0.17) across a 4-fold range (5% to 20%) of current (Fig. S1d). Only when the variance was substantially large did stimulus σ result in effects on cell reliability.

K Nearest Neighbor Analysi

The K nearest neighbor (Knn) approach was used to classify the 589 spike trains from 15 conditions in 8 cells. The same input stimulus was given to all cells with different DC offsets to induce firing over multiple trials (N = 30-40). For computational efficiency, analysis was performed in the space of the first 15 principal components and because classification accuracy did not change for principal components > 10. The original data was then broken up into testing and training sets. The testing sets established the location of known responses in the principal component space, and the training set was probed with respect to these known responses. The Euclidian distance of the unknown response to all known responses was then calculated and the N nearest neighbors were used to determine what cell/condition the unknown spike response belonged to. This process of generating testing and training sets was repeated 20 times with each repeat reflecting a different random population of testing and training to ensure that the classification accuracy was not due to artifacts of selecting a single testing/training population.

Information calculation

To generate population responses for our entropy calculations to an identical stimulus, a random group of mitral cells was selected from all the neurons that received the identical input stimulus. Each of these different populations was considered a single diverse mitral cell population. When homogeneous populations were made, spikes drawn at random from a *single* recorded neurons was assigned for all the cells in the population,. When homogeneous populations were generated, random sampling was done with replacement.

Spike trains were then binned into non-overlapping bins of various sizes. If one or more spikes occurred in a bin, then a value of 1 was recorded in that bin. If no spikes occurred in the bin, then a value of 0 was placed in this bin. In bin sizes as large as 12 ms, no examples of bins containing two or more spikes could be found, ensuring that at these bin sizes, the binary strings of 1s and 0s captured the entire spike train. In bins of size 16 ms, 2.8% of the bins had more than one spike, and therefore only time bins of up to 12 ms were considered to ensure that no relevant information was lost in our entropy calculations as a result of doublet spikes.

Supplementary Material

Refer to Web version on PubMed Central for supplementary material.

Acknowledgments

We wish to thank Gregory M. LaRocca for assistance with the immunohistochemistry and, Brett Benedetti, Dr. Alison Barth, Dr. Jason Castro, and members of the Urban lab for helpful comments on this manuscript. Funding was provided by NIDCD (R01DC0005798).

Reference List

1. Ramon YC. Structure and connections of neurons. Bull Los Angel Neuro Soc. 1952; 17:5–46. [PubMed: 14944970]
2. Marder E, Goaillard JM. Variability, compensation and homeostasis in neuron and network function. Nat Rev Neurosci. 2006; 7:563–574. [PubMed: 16791145]
3. Gupta A, Wang Y, Markram H. Organizing principles for a diversity of GABAergic interneurons and synapses in the neocortex. Science. 2000; 287:273–278. [PubMed: 10634775]
4. Mainen ZF, Sejnowski TJ. Influence of dendritic structure on firing pattern in model neocortical neurons. Nature. 1996; 382:363–366. [PubMed: 8684467]
5. Schaefer AT, Larkum ME, Sakmann B, Roth A. Coincidence detection in pyramidal neurons is tuned by their dendritic branching pattern. J Neurophysiol. 2003
6. Schulz DJ, Goaillard JM, Marder E. Variable channel expression in identified single and electrically coupled neurons in different animals. Nat Neurosci. 2006; 9:356–362. [PubMed: 16444270]
7. Ecker AS, et al. Decorrelated neuronal firing in cortical microcircuits. Science. 2010; 327:584–587. [PubMed: 20110506]
8. Friedrich RW, Laurent G. Dynamic optimization of odor representations by slow temporal patterning of mitral cell activity. Science. 2001; 291:889–894. [PubMed: 11157170]
9. Stocks NG. Suprathreshold stochastic resonance in multilevel threshold systems. Phys Rev Lett. 2000; 84:2310–2313. [PubMed: 11018872]
10. Brody CD, Hopfield JJ. Simple networks for spike-timing-based computation, with application to olfactory processing. Neuron. 2003; 37:843–852. [PubMed: 12628174]

11. Ermentrout GB, Galan RF, Urban NN. Reliability, synchrony and noise. Trends Neurosci. 2008; 31:428–434. [PubMed: 18603311]
12. Chen TW, Lin BJ, Schild D. Odor coding by modules of coherent mitral/tufted cells in the vertebrate olfactory bulb. Proc Natl Acad Sci U S A. 2009; 106:2401–2406. [PubMed: 19181842]
13. Mombaerts P, et al. Visualizing an olfactory sensory map. Cell. 1996; 87:675–686. [PubMed: 8929536]
14. Wachowiak M, Denk W, Friedrich RW. Functional organization of sensory input to the olfactory bulb glomerulus analyzed by two-photon calcium imaging. Proc Natl Acad Sci U S A. 2004; 101:9097–9102. [PubMed: 15184670]
15. Wellis DP, Scott JW, Harrison TA. Discrimination among odorants by single neurons of the rat olfactory bulb. J Neurophysiol. 1989; 61:1161–1177. [PubMed: 2746317]
16. Margrie TW, Sakmann B, Urban NN. Action potential propagation in mitral cell lateral dendrites is decremental and controls recurrent and lateral inhibition in the mammalian olfactory bulb. Proc Natl Acad Sci U S A. 2001; 98:319–324. [PubMed: 11120888]
17. Kazama H, Wilson RI. Origins of correlated activity in an olfactory circuit. Nat Neurosci. 2009; 12:1136–1144. [PubMed: 19684589]
18. Renart A, et al. The asynchronous state in cortical circuits. Science. 2010; 327:587–590. [PubMed: 20110507]
19. Schoppa NE, Westbrook GL. Regulation of synaptic timing in the olfactory bulb by an A-type potassium current. Nat Neurosci. 1999; 2:1106–1113. [PubMed: 10570488]
20. Chen WR, Shepherd GM. Membrane and synaptic properties of mitral cells in slices of rat olfactory bulb. Brain Res. 1997; 745:189–196. [PubMed: 9037409]
21. de Ruyter van Steveninck RR, Lewen GD, Strong SP, Koberle R, Bialek W. Reproducibility and variability in neural spike trains. Science. 1997; 275:1805–1808. [PubMed: 9065407]
22. Mainen ZF, Sejnowski TJ. Reliability of spike timing in neocortical neurons. Science. 1995; 268:1503–1506. [PubMed: 7770778]
23. Galan RF, Ermentrout GB, Urban NN. Optimal time scale for spike-time reliability: theory, simulations, and experiments. J Neurophysiol. 2008; 99:277–283. [PubMed: 17928562]
24. Ermentrout GB, Galan RF, Urban NN. Relating neural dynamics to neural coding. Phys Rev Lett. 2007; 99:248103. [PubMed: 18233494]
25. Bryant HL, Segundo JP. Spike initiation by transmembrane current: a white-noise analysis. J Physiol. 1976; 260:279–314. [PubMed: 978519]
26. Schwartz O, Pillow JW, Rust NC, Simoncelli EP. Spike-triggered neural characterization. J Vis. 2006; 6:484–507. [PubMed: 16889482]
27. Meister M, Pine J, Baylor DA. Multi-neuronal signals from the retina: acquisition and analysis. J Neurosci Methods. 1994; 51:95–106. [PubMed: 8189755]
28. Geffen MN, Broome BM, Laurent G, Meister M. Neural encoding of rapidly fluctuating odors. Neuron. 2009; 61:570–586. [PubMed: 19249277]
29. Osborne LC, Palmer SE, Lisberger SG, Bialek W. The neural basis for combinatorial coding in a cortical population response. J Neurosci. 2008; 28:13522–13531. [PubMed: 19074026]
30. Wesson DW, Verhagen JV, Wachowiak M. Why sniff fast? The relationship between sniff frequency, odor discrimination, and receptor neuron activation in the rat. J Neurophysiol. 2009; 101:1089–1102. [PubMed: 19052108]
31. Verhagen JV, Wesson DW, Netoff TI, White JA, Wachowiak M. Sniffing controls an adaptive filter of sensory input to the olfactory bulb. Nat Neurosci. 2007; 10:631–639. [PubMed: 17450136]
32. Schaefer AT, Angelo K, Spors H, Margrie TW. Neuronal oscillations enhance stimulus discrimination by ensuring action potential precision. PLoS Biol. 2006; 4:e163. [PubMed: 16689623]
33. Wang Y, et al. Heterogeneity in the pyramidal network of the medial prefrontal cortex. Nat Neurosci. 2006; 9:534–542. [PubMed: 16547512]

34. Day M, et al. Dendritic excitability of mouse frontal cortex pyramidal neurons is shaped by the interaction among HCN, Kir2, and Kleak channels. J Neurosci. 2005; 25:8776–8787. [PubMed: 16177047]
35. Taylor AL, Goaillard JM, Marder E. How multiple conductances determine electrophysiological properties in a multicompartment model. J Neurosci. 2009; 29:5573–5586. [PubMed: 19403824]
36. Goaillard JM, Taylor AL, Schulz DJ, Marder E. Functional consequences of animal-to-animal variation in circuit parameters. Nat Neurosci. 2009; 12:1424–1430. [PubMed: 19838180]
37. Sugino K, et al. Molecular taxonomy of major neuronal classes in the adult mouse forebrain. Nat Neurosci. 2006; 9:99–107. [PubMed: 16369481]
38. Wang Y, Gupta A, Toledo-Rodriguez M, Wu CZ, Markram H. Anatomical, physiological, molecular and circuit properties of nest basket cells in the developing somatosensory cortex. Cereb Cortex. 2002; 12:395–410. [PubMed: 11884355]
39. Chou YH, et al. Diversity and wiring variability of olfactory local interneurons in the Drosophila antennal lobe. Nat Neurosci. 2010; 13:439–449. [PubMed: 20139975]
40. Desai NS, Rutherford LC, Turrigiano GG. Plasticity in the intrinsic excitability of cortical pyramidal neurons. Nat Neurosci. 1999; 2:515–520. [PubMed: 10448215]
41. Salinas E, Sejnowski TJ. Correlated neuronal activity and the flow of neural information. Nat Rev Neurosci. 2001; 2:539–550. [PubMed: 11483997]
42. Arevian AC, Kapoor V, Urban NN. Activity-dependent gating of lateral inhibition in the mouse olfactory bulb. Nat Neurosci. 2008; 11:80–87. [PubMed: 18084286]
43. Laurent G, et al. Odor encoding as an active, dynamical process: experiments, computation, and theory. Annu Rev Neurosci. 2001; 24:263–297. [PubMed: 11283312]
44. Bazhenov M, et al. Model of transient oscillatory synchronization in the locust antennal lobe. Neuron. 2001; 30:553–567. [PubMed: 11395014]
45. Stopfer M, Bhagavan S, Smith BH, Laurent G. Impaired odour discrimination on desynchronization of odour-encoding neural assemblies. Nature. 1997; 390:70–74. [PubMed: 9363891]
46. Galan RF, Fourcaud-Trocme N, Ermentrout GB, Urban NN. Correlation-induced synchronization of oscillations in olfactory bulb neurons. J Neurosci. 2006; 26:3646–3655. [PubMed: 16597718]
47. Kashiwadani H, Sasaki YF, Uchida N, Mori K. Synchronized oscillatory discharges of mitral/tufted cells with different molecular receptive ranges in the rabbit olfactory bulb. J Neurophysiol. 1999; 82:1786–1792. [PubMed: 10515968]
48. Kapoor V, Urban NN. Glomerulus-specific, long-latency activity in the olfactory bulb granule cell network. J Neurosci. 2006; 26:11709–11719. [PubMed: 17093092]
49. Urban NN, Sakmann B. Reciprocal intraglomerular excitation and intra- and interglomerular lateral inhibition between mouse olfactory bulb mitral cells. J Physiol. 2002; 542:355–367. [PubMed: 12122137]

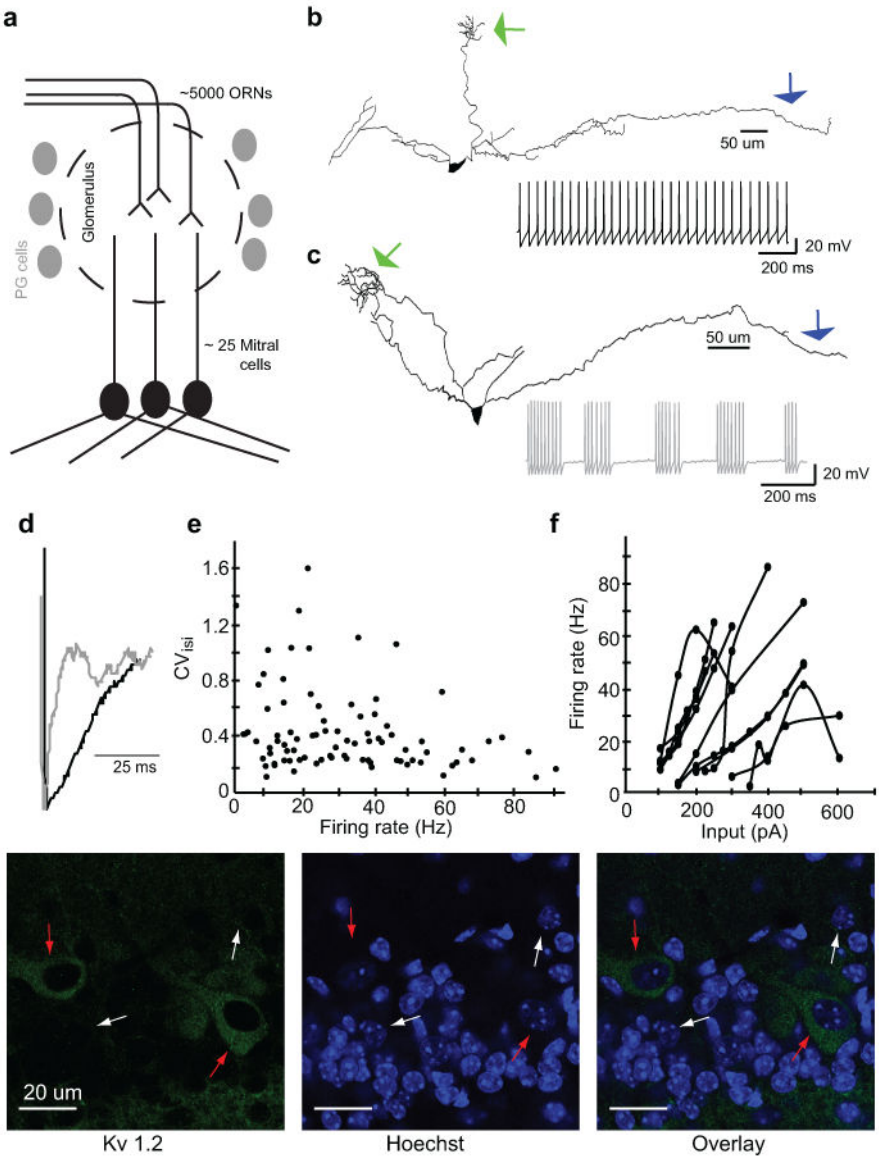

Fig 1.

Intrinsic diversity of mitral cell populations. **a)** Schematic of mammalian main olfactory bulb circuitry. Olfactory receptor neurons (ORNs) expressing one olfactory receptor all send their axons to the same glomerulus. All mitral/tufted (M/T) cell apical dendrites connected to a glomerulus receive inputs that are highly correlated. **b-c**) Biocytin fills of two representative mitral cells with spike responses to a fixed DC current. In both cells, apical dendrites and their tufts (green arrow) and lateral dendrites (blue arrow) are intact in the slice. **d)** Mitral cell spike outputs are also diverse based on the shape of the after hyperpolarizations that follow their action potentials (color corresponds to traces in b-c). **e)** Mitral cells differ widely in both firing rates and in the coefficients of variation (CVs) of their interspike intervals. **f)** Recordings of mitral cells show wide variation in excitability as described by the frequency of action potentials generated by constant current stimuli of different amplitudes. **g)** Confocal micrographs of the olfactory bulb stained for Kv1.2

(green, left panel) and Hoechst (blue, middle panel) and an overlay of Kv1.2 positive cell bodies and mitral cell nuclei (right panel). Red arrows highlight cell bodies of Kv positive neurons and their nuclei while white arrows highlight nuclei of mitral cells that do not express Kv1.2. Kv positive and negative mitral cells are interspersed in the same focal plane.

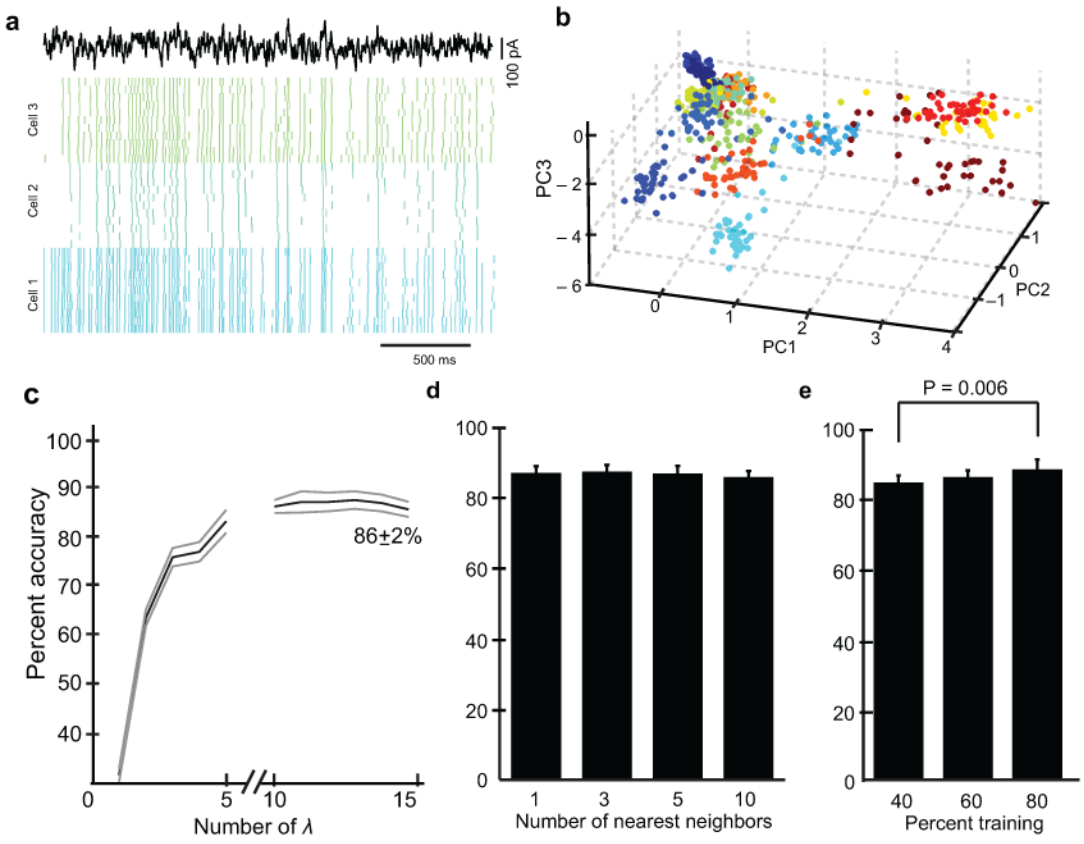

Fig 2.

Uniqueness of mitral cell output to identical input. **a)** Spike rasters of 10 trials for three mitral cells to an identical fluctuating input (top black trace). **b)** Projection of all spike patterns (points) from multiple cells (colors) onto a space defined by the first 3 principal components calculated from all spike trains. **c)** Classification accuracy of spike trains based on recording identity as a function of the number of eigenvectors (λ) used for classification. **d)** The number of nearest neighbours (1, 3, 5, 10) does not affect the classification accuracy. **e)** The percentage of trials used in the testing and the training sets affects the classification accuracy only when 80% of spike trains are used in training. (error = s.d.)

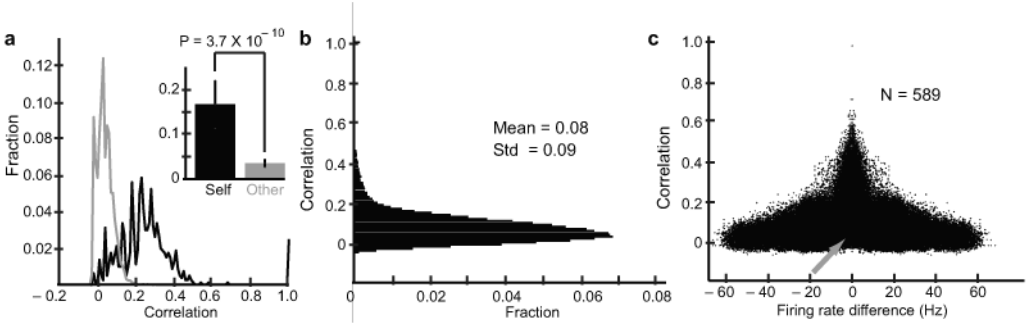

Fig. 3.

Intrinsic diversity affects pairwise spike train correlations. **a)** Histogram of all pairwise correlations for within-cell (black) and between-cell spike trains (red). **Inset**. Mean pairwise correlations are significantly different within-cells and between cells. **b)** Histogram of all pairwise correlations from cells receiving an identical input. **c)** Pairwise correlations of all spike trains from all mitral cells as a function of differences in firing rates. (Error = s.d.)

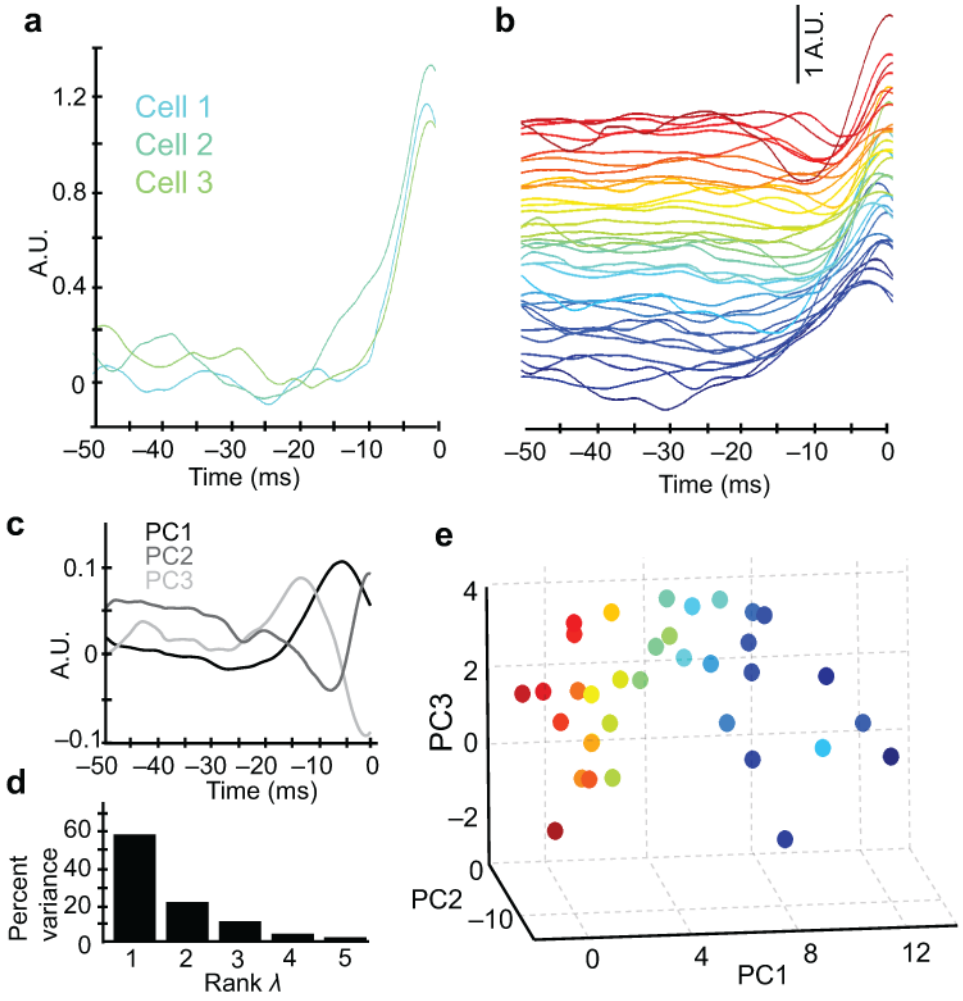

Fig 4.

Mitral cell spike triggered average (STA) diversity. **a)** Spike-triggered averages (STA) for the three cells in Fig 3a. **b)** STAs for a population of mitral cells that all received noisy input illustrates the diversity (N = 35 STAs). Color corresponds to identity in e. **c)** Principal components (PC) 1-3 of the STAs in b. **d)** Variance explained by the 1st 5 principal components for this population of mitral cells. **e)** Projection of each STA onto the space of principal components in c shows mitral cell STAs are not uniformly distributed, but span an arc in the space.

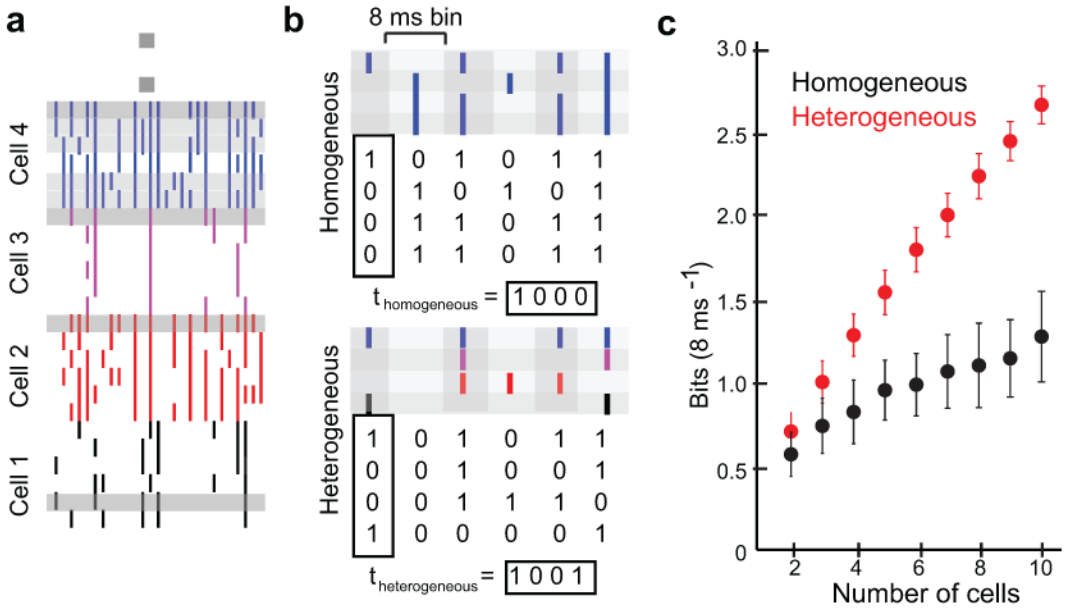

Fig 5.

Heterogeneous populations of mitral cells carry more information than their homogeneous counterparts. **a)** Representative trials of spike trains (6/cell) from 4 mitral cells all given an identical fluctuating input. **b)** A homogeneous population response was constructed by randomly drawing spike trains from a single recorded cell (blue). A heterogeneous population was constructed by randomly drawing spike trains from different neurons. The responses of each population were binarized into words of 0s and 1s and the pattern of words, for instance $t_{homogeneous}$ and $t_{heterogeneous}$, were analyzed to calculate information. **c)** Heterogeneous populations of mitral cells carry twice as much information as homogeneous populations of cells. (Error = s.d.)

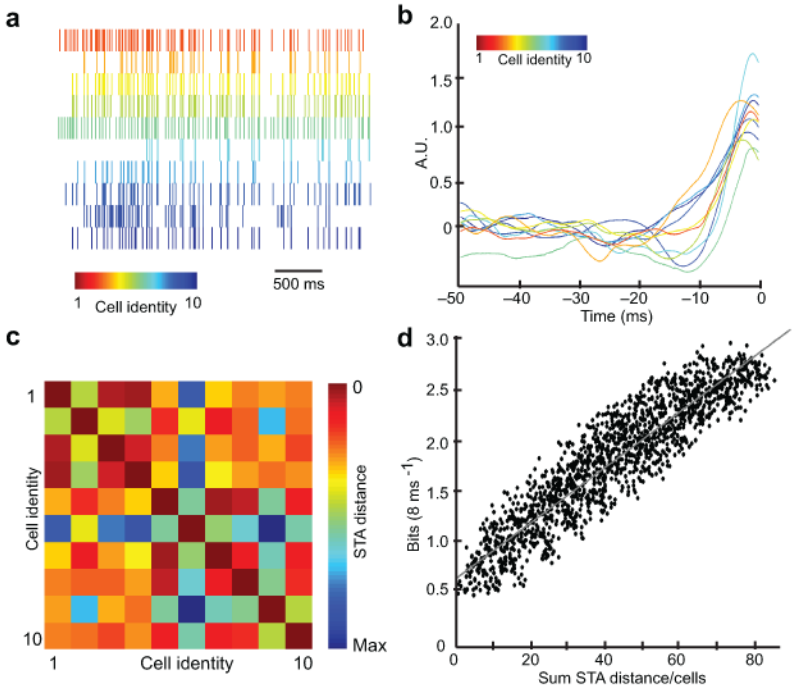

Fig. 6.

Biophysical diversity correlates to information transfer. **a)** Spike train examples of a single trial for 10 mitral cells with different STAs. **b)** STAs of the 10 cells in (a) colour coded by cell identity. **c)** STA distance matrix calculated by measuring the Euclidian distance of the STAs to one another in the space defined by the principal components. **d)** Bits of information as a function of sum of STA distance/number of cells.

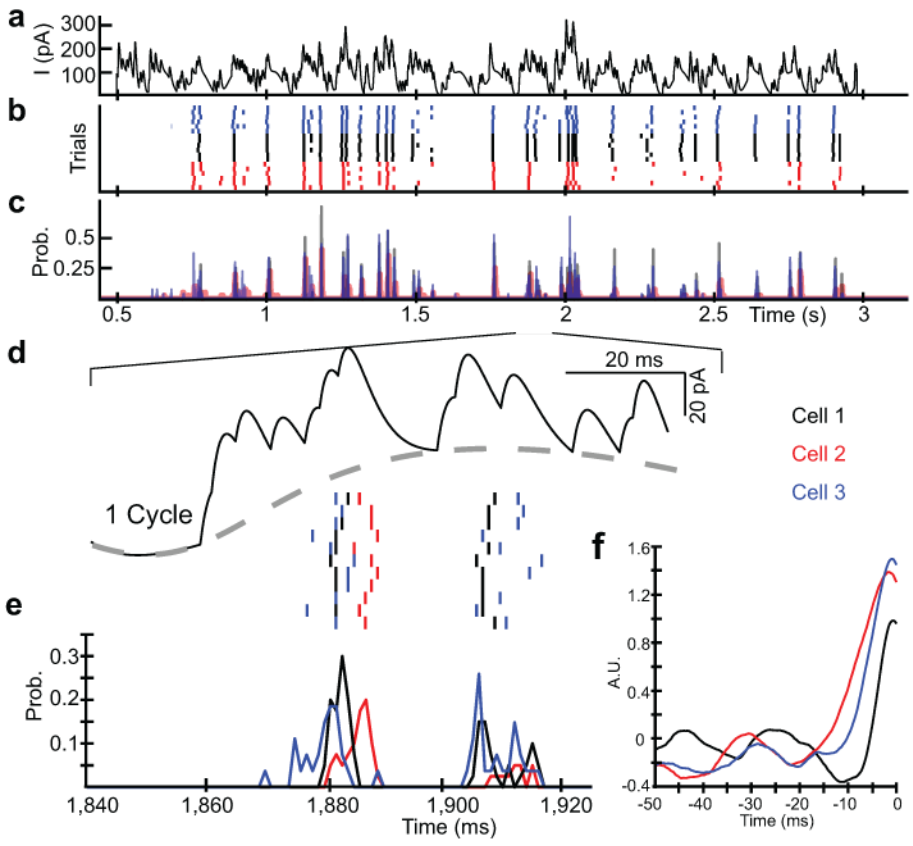

Fig. 7.

Heterogeneous populations improve the coding of physiologically relevant stimuli. **a)** Synaptic input currents modulated by an 8 Hz periodic oscillation. **b)** Responses of 6 trials each from 3 mitral cells to the identical periodic input. **c)** Probability of spike firing at various stimulus epochs. **d)** Enlargement of one theta cycle and spike times for the three cells in b over multiple trials and the **e)** probability of firing during the cycle. **f)** STAs for the 3 mitral cells calculated by injecting a rapidly fluctuating noisy input.